Case Studies in Thermal Engineering 27 (2021) 101314

Contents lists available at ScienceDirect

Case Studies in Thermal Engineering

journal homepage: www.elsevier.com/locate/csite

Thermo-economic, exergetic and mechanical analysis of thermoelectric generator with hollow leg structure; impact of leg cross-section shape and hollow-to-filled area ratio

Min Li [a], Hamed Sadighi Dizaji [b], Soheil Asaadi [b], Fahd Jarad [c,d,**], Ali E. Anqi [e], Makatar Wae-hayee [f,*]

[a] Institute of Applied Economics, Yango University, Fuzhou, 350015, China
[b] Department of Mechanical Engineering, Urmia University, Urmia, Iran
[c] Department of Mathematics, Cankaya University, Ankara, Turkey
[d] Department of Medical Research, China Medical University Hospital, Taichung, Taiwan
[e] Department of Mechanical Engineering, College of Engineering, King Khalid University, Abha, 61421, Saudi Arabia
[f] Department of Mechanical Engineering, Faculty of Engineering, Prince of Songkla University, Hatyai, Songkhla, 90110, Thailand

GRAPHICAL ABSTRACT

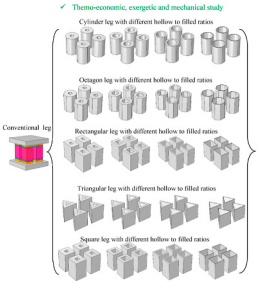

ARTICLE INFO

Keywords:
Thermoelectric generator
Economic
Seebeck
Hollow leg

ABSTRACT

Filled square cross-section shape is the common conventional structure for n-type and p-type legs of thermoelectric generators. However, other cross-section shapes with hollow structure can significantly increase the output power of thermoelectric generator. However, mechanical strength and economic considerations may still remain as the significant challenges and factors. Hence, in this research, different hollow cross-section leg shapes are investigated for

* Corresponding author.
** Corresponding author. Department of Mathematics, Cankaya University, Ankara, Turkey.
E-mail addresses: fahd@cankaya.edu.tr (F. Jarad), wmakatar@eng.psu.ac.th (M. Wae-hayee).

https://doi.org/10.1016/j.csite.2021.101314
Received 5 June 2021; Received in revised form 1 August 2021; Accepted 5 August 2021
Available online 6 August 2021

thermoelectric generator from all thermal, economic, exergetic and mechanical viewpoints simultaneously through a 3D validated numerical simulation. Output voltage/power, energy-efficiency, exergy efficiency, Von-Mises stress, and the dollar/watt value are calculated for all mentioned structures and optimum conditions are identified. As a sample result, the triangular shape leg is able to generate up to 100% more power and better conversion/exergy efficiency (compared to the rectangular) at maximum input heat flux while mechanically less reliable design. Many other remarkable and interesting findings are provided in this manuscript.

Nomenclature:

A	differential operator
B	Thermo-elastic coefficient
β	coefficients of thermal expansions, (K^{-1})
C_p	specific heat at constant pressure $(Jkg^{-1}K^{-1})$
C_v	specific heat at constant volume $(Jkg^{-1}K^{-1})$
D	electric displacement (Cm^{-1})
[D]	stiffness matrix
E	electric field intensity, (Vm^{-1})
f	volume force (Nm^{-3})
H	height, (mm)
I	electric current, (A)
J	electric current density, (Am^{-2})
k	thermal conductivity, $(Wm^{-2}K^{-1})$
W	width, (mm)
P_{out}	power output, (W)
P_l	pitch, (mm)
Q_{in}	heat input, (W)
R	electrical resistance, (Ω)
R_A	ratio of inner hollow area to total area
R_H	height ratio of legs
R_L	load resistance, (Ω)
T	temperature, (K)
T_k	kelvin reference temperature, (K)
S	stress, (Pa)
u	displacement, (mm)

Greek letters

α	Seebeck coefficient, (VK^{-1})
η	conversion efficiency
Δ	difference
ρ	density, (kgm^{-3})
σ	electrical conductivity, (Sm)
ε	strain vector
ζ	exergy efficiency

subscript

0	environment
c	cold side
cr	ceramic
h	hot side
ic	interconnector

1. Introduction

The increasing demands for energy and many environmental issues caused by the excessive use of conventional sources of energy such as fossil fuels have shifted the attention of the researchers toward renewable energy studies in recent years. In addition to improving the methods of utilization of the renewable energy resources, clean energy conversion technologies such as thermoelectric generators have provided opportunities to harvest the wasted energy from power plants, motor vehicles, etc.

Many studies have been conducted on thermoelectric generators with the aim of geometrical optimization [1–3]. The previous investigations proved that thermoelectric module structure and geometry have a significant impact on the performance of the device and therefore the design limitations and considerations are required [4]. The following section summarizes the main findings in the field of thermoelectric generator efficiency enhancement with pin and leg shape optimization.

Sahin and Yilbas [5] performed a theoretical investigation and formulated the output power and efficiency of the thermoelectric generators with varying leg shapes. For a range of studied hot side temperatures and external load resistances, it was found that the shape parameter has a favorable effect on the efficiency. However, the shape parameter had an inverse effect on the output power. The influence of pin geometry on thermal stress and thermodynamic performance of a thermoelectric generator was studied by Al-Merbati et al. [6]. They evaluated the stress and temperature fields in the device with the finite element method. Results indicated that the lifespan of the device can be improved with a geometric design of pins. Besides, the effect of the pin area ratio of the hot junction to the cold junction was considered in the simulations and optimized values were presented. Lamba and Kausik [7] carried out a thermodynamic analysis on the performance of a thermoelectric generator considering the influence of the Thomson effect and leg geometry configuration. The analytical expressions of output power, energy efficiency, exergy efficiency, and dimensionless figure of merit were derived. For the trapezoidal shape, results proved that the increase of shape parameter enhances the energy and exergy efficiency but has an inverse impact on the output power. The optimum values for shape parameter and external load ratio to attain the maximum output power were determined to be 1 and 2. Yilbas et al. [8] performed thermal and stress finite element analyses on a horizontal thermoelectric generator considering rectangular and tapered pin configurations. Results indicated that hot and cold side junctions are subjected to the highest values of von Mises stress. Moreover, it was founded that tapered pin configuration reduces the thermal stress compared to rectangular pin configuration. Other studies [9–14] also tried to optimize the thermoelctric generator from different viewpoints including strees analysis, proposition of hybrid systems, phase change material, solar applications, etc.

Thimont and LeBlanc [15] performed a numerical study on the output power and thermal resistance of thermoelectric generators with various leg geometries. They considered hollow geometries with rectangular, triangular, and circular cross-sections. A numerical finite element investigation on the thermo-mechanical performance of thermoelectric devices with coaxial and rotated leg geometries was conducted by Ertrun and Mossi [16]. They considered the elastoplastic behavior and the temperature dependency of materials and proved that the models with coaxial legs generated less power but had higher efficiency values compared to conventional models.

One of the significant effective factor on the performance of thermoelectric generator is the internal resistance of the generator which is due to the internal resistance of the legs. Filled shape legs causes higher internal resistance because of more material existence. The parameter $R_A = \frac{A_L}{A_0}$ is defined for hollow leg structure Where A_0 is the base area of shapes in filled condition and A_i is the area of the inner hollow section. For instance the $R_A = 0.9$ corresponds to a study case in which 90% of leg volume is cut from inside. With the increase of R_A, the internal resistance of the system decreases because it has an inverse relation with the cross-sectional area of the legs. That is why hollow leg is able to provide more power output. Besides, as hollow leg uses less material, it has economic benefit as well.

Briefly, many researchers have investigated the thermoelectric and mechanical performance of thermoelectric generators with different geometries of legs in traditional filled solid shapes. However, extremely few studies cover the performance analyses of thermoelectric generators with hollow structures. Particularly, simultaneous energy, exergy, mechanical and economic evaluations are required for such complicated hollow structures with different cross-sections and different hollow to filled ratios. Hence in this paper, the power generation, energy efficiency, exergy efficiency, mechanical reliability, and cost analysis of thermoelectric generators with ring shape legs considering various cross-sectional shapes are simultaneously investigated.

2. Numerical methods

2.1. Model structure and materials

In general, a three-dimensional model of a thermoelectric generator with 4 ring shape semiconductor legs (2 n-type and 2 p-type) which are connected by copper interconnectors is employed. Thin wielding layers made of solder are considered between the legs and copper interconnectors. Two ceramic insulator layers are attached to the cold and hot sides of the thermoelectric generator. The bottom surface of thermoelectric is considered to be the heat source while the top surface acts as the heat sink. The schematic of the thermoelectric generator and all basic geometries are depicted in Fig. 1(a). Five different geometric shapes including circular, square, octagonal, rectangular, and triangular are considered for the design of thermoelectric legs which are illustrated Fig. 1 (b). A proportion of the cross-sectional area is cut from the inside of the thermoelectric legs which forms ring shape legs. The geometric design of the thermoelectric generator is implemented in a way that the base cross-sectional area (A_0) in all shapes are kept at $1mm^2$ and so the volume of legs does not vary between shapes. Ratio of inner hollow area to total area ($R_A = \frac{A_i}{A_0}$) for all shapes is 0.5 (unless other indicated). A detailed presentation of thermoelectric legs in ring shape geometry is shown in Fig. 1 (b) including geometry. Bi2Te3 is selected for the n-type and p-type pins. The properties of Bi2Te3 are considered to be temperature-dependent to increase the precision of simulations. The elastoplastic behaviour of wielding layers and copper interconnectors are included in the analysis because this

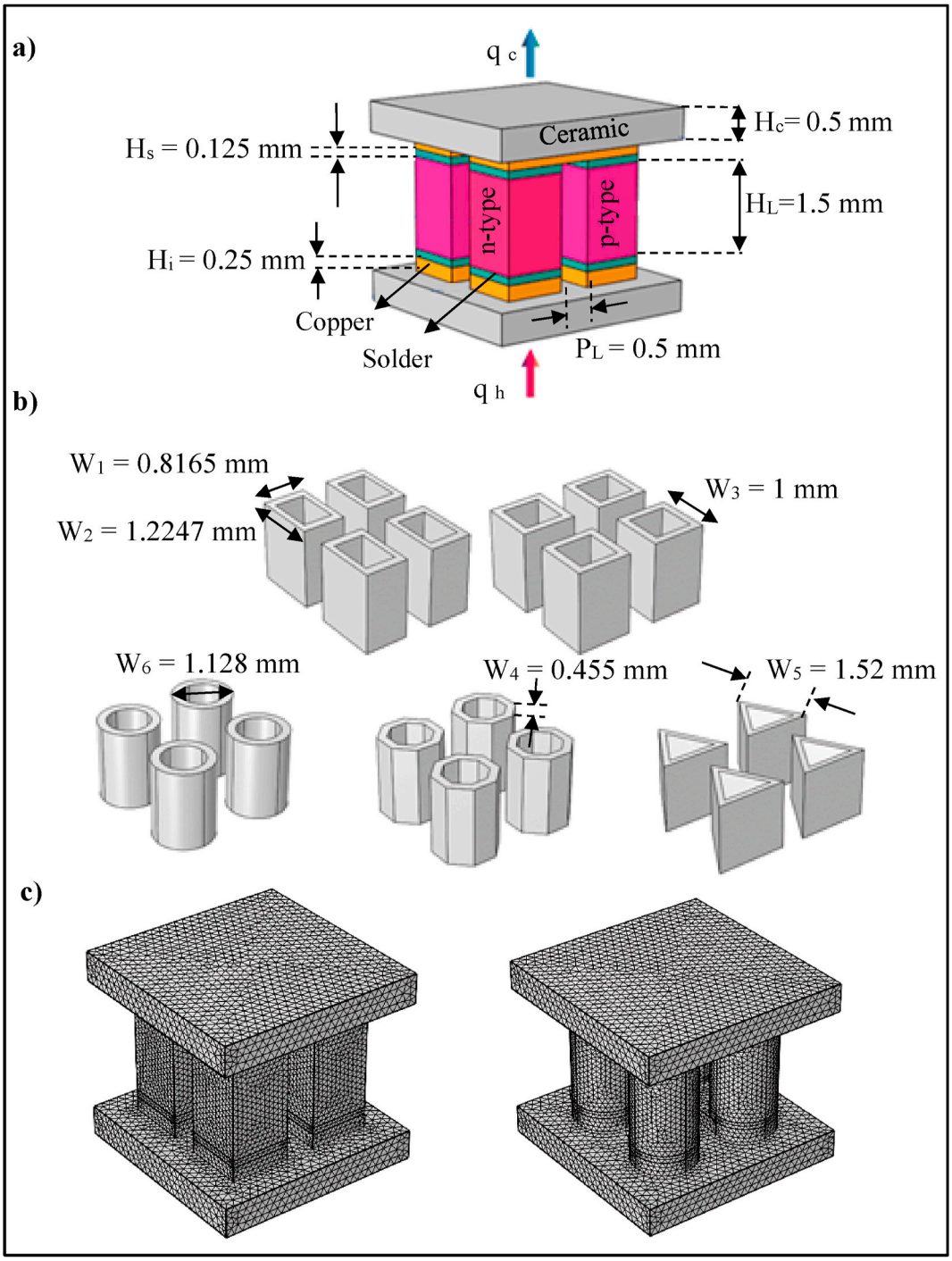

Fig. 1. a) The schematic of thermoelectric generator and its dimensions, b) Various considered cross-sections of ring legs and their geometries, c) a sample general view of the mesh.

Table 1
Properties of Bi_2Te_3 elements [18].

Properties	Bi_2Te_3 (n-type)	Bi_2Te_3 (p-type)
k $(Wm^{-2}K^{-1})$	$2.24\times10^{-8}(T-T_0)^3+7.09\times10^{-6}(T-T_0)^2-1.26\times10^{-2}(T-T_0)+4.09$	$-3.31\times10^{-8}(T-T_0)^3+7.29\times10^{-5}(T-T_0)^2-3.79\times10^{-2}(T-T_0)+7.12$
α(VK^{-1})	$1.46\times10^{-11}(T-T_0)^3-1.50\times10^{-8}(T-T_0)^2+5.14\times10^{-6}(T-T_0)-8.12\times10^{-4}$	$-2.96\times10^{-11}(T-T_0)^3+3.11\times10^{-8}(T-T_0)^2-1.08\times10^{-5}(T-T_0)+1.48\times10^{-3}$
R (Ωm)	$-2.13\times10^{-13}(T-T_0)^3+1.42\times10^{-10}(T-T_0)^2+1.09\times10^{-8}(T-T_0)-2.1\times10^{-6}$	$-7.60\times10^{-13}(T-T_0)^3+7.78\times10^{-10}(T-T_0)^2-1.93\times10^{-7}(T-T_0)+1.8\times10^{-5}$
$\vec{\beta}(K^{-1})$	$-3.408\times10^{-16}(T-T_0)^4+9.317\times10^{-13}(T-T_0)^3-9.246\times10^{-10}(T-T_0)^2+3.96\times10^{-7}(T-T_0)-4.894\times10^{-5}$	$-3.408\times10^{-16}(T-T_0)^4+9.317\times10^{-13}(T-T_0)^3-9.246\times10^{-10}(T-T_0)^2+3.96\times10^{-7}(T-T_0)-4.894\times10^{-5}$
Young Modulus (Pa)	$1.667(T-T_0)^4-2.667\times10^3(T-T_0)^3+1.533\times10^6(T-T_0)^2-3.883\times10^8(T-T_0)+1\times10^{11}$	$1.667(T-T_0)^4-2.667\times10^3(T-T_0)^3+1.533\times10^6(T-T_0)^2-3.883\times10^8(T-T_0)+1\times10^{11}$
Density (Kgm^{-3})	7740	7740
Poisson's ratio	0.23	0.23

behaviour can have a relaxing effect which leads to the reduction of thermal stress in the thermoelectric legs [3,16,17]. The material properties of semiconductors, interconnectors, insulators, and wielding layers are listed in Table 1 and Table 2.

2.2. Governing equations and boundary conditions

The thermoelectric phenomena are defined by interacting and coupled thermal and electrical fields including Peltier, Fourier, Joule, and Thomson effects. A set of partial differential equations are required to describe the multi-physics fields like the thermoelectric effect. Main equations are provided as Eq. (1) [19,20]. The general coupled equations of thermoelectric effect are given by combinations of Eq (1.1) to (1.5) as Eq. (2). The time derivatives in all the above equations are eliminated in the steady-state condition. To evaluate the mechanical stress and displacement caused by thermal load and temperature gradient Eq. (3) is required.

$$\begin{cases} \textit{heat energy transfer}: \rho c_p\dfrac{\partial T}{\partial t}+\nabla.\vec{q}=\dot{q} \quad (1.1)\\ \textit{electric current continuity}: \nabla.\left(\vec{J}+\dfrac{\partial\vec{D}}{\partial t}\right)=0 \quad (1.2)\\ \textit{Joule heat}: \dot{q}=\vec{J}.\vec{E} \quad (1.3)\\ \textit{heat flux}: \vec{q}=-k\nabla T+\alpha T\vec{J} \quad (1.4)\\ \textit{electric current density}: \vec{q}=-k\nabla T+\alpha T\vec{J} \quad (1.5) \end{cases} \tag{1}$$

$$\rho C_p\frac{\partial T}{\partial t}+\nabla.(-k\nabla T-\alpha T(\sigma\nabla V+\sigma\alpha\nabla T))=(-\sigma\nabla V-\sigma\alpha\nabla T).(-\nabla V) \tag{2}$$

$$\begin{cases} A\vec{S}+f=0 \quad (3.1)\\ \vec{\varepsilon}=A\vec{u} \quad (3.2) \end{cases} \tag{3}$$

where $[A]$ stands for the differential operator, $\vec{S}$ is stress vector, $\vec{\varepsilon}$ is strain vector, f is volume force, and $\vec{u}$ is the displacement vector.

Table 2
Properties of copper interconnectors, wielding and ceramic layers [18].

Properties	Copper	Ceramic layers	Wielding layers
k $(Wm^{-2}K^{-1})$	385	25	55
R (Ωm)	1.69×10^{-7}	1×10^{12}	5×10^{-8}
$\vec{\beta}(K^{-1})$	1.7×10^{-5}	0.68×10^{-5}	2.7×10^{-5}
Young Modulus (Pa)	12×10^{10}	34×10^{10}	4.45×10^{10}
Yielding stress (Pa)	7×10^{10}	–	2.6×10^{10}
Tangential modulus (Pa)	2.4×10^{10}	–	2.4×10^{10}
Density (Kgm^{-3})	8930	3970	7240
Poisson's ratio	0.3	0.22	0.33

The thermo-mechanical behavior of thermoelectric generator can be evaluated via the combination of thermal and mechanical fields as Eq. (4).

$$\begin{cases} \overrightarrow{S} = [D]\overrightarrow{\varepsilon} - \overrightarrow{B}\Delta T \quad (4.1) \\ Q = T_k B^T \varepsilon + \rho c_v \Delta T \quad (4.2) \\ \overrightarrow{B} = [D]\overrightarrow{\beta} \quad (4.3) \end{cases} \tag{4}$$

where $\vec{B}$ is thermo-elastic coefficient vector and $\vec{\beta}$ is thermal expansion coefficient vector. To solve the electric and thermo-mechanical coupled equations a set of boundary conditions with some assumptions are considered listed as follow:

- Thomson effect is included in the analyses.
- Contact resistances in the thermal and electrical forms are ignored.
- Mechanical support (fixed) boundary condition is applied on the upper (cold) side of the thermoelectric device.
- The bottom and upper surfaces are heat source and heat sink boundaries while all other boundaries are thermally insulated.
- A constant temperature of 25°C is employed on the cold side. Heat is input to the device on the hot side by a heat flux boundary condition. The ambient temperature T_0 is 20°C.
- An electrical ground boundary condition is applied to one end of the thermocouple.

2.3. Parameter definition

The results of this paper are presents by energy, exergy, and cost parameters. The required parameters are presented as Eq. (5) [20] in which Q_{in} is the heat input, R is internal electrical resistance and R_L is the external load resistance. The maximum power generation and efficiency can be obtained when $R = R_L$ [21]. The exergy efficiency of the thermoelectric generator is described by the ratio of the output power to the input fuel where the fuel represents the exergy stream expended to generate the power and can be written as Eq. (6) [22,23].

The comprehensive analyses of any power generation system require close attention to the price of net output power which indicates the true value of the system in practical conditions. The dollar/watt ($/W) value takes into account the capital investment on the materials used in the thermoelectric system and defines a proportionality between the energy efficiency of the system and volumetric costs of materials [24–26]. Where V_m is the material volume and C_m is the volumetric cost respectively.

$$\begin{cases} open-circuit\ voltage : V_{oc} = \alpha\Delta T \quad (5.1) \\ electric\ current : I = \dfrac{\alpha\Delta T}{R_L + R} \quad (5.2) \\ output\ power : \left(\dfrac{\alpha\Delta T}{R_L + R}\right)^2 \times R_L \quad (5.3) \\ energy\ efficiency : \eta = \dfrac{P_{out}}{Q_{in}} \quad (5.4) \end{cases} \tag{5}$$

$$\begin{cases} \zeta = \dfrac{\text{Exergy Out}}{\text{Exergy in}} = \dfrac{P_{out}}{Ex_{in}} \quad (6.1) \\ Ex_{in} = Q_{in}\left(1 - \dfrac{T_0}{T_h}\right) \quad (6.2) \end{cases} \tag{6}$$

$$\left(\frac{\$}{W}\right) \sim \left(\frac{V_m}{P_{out}}\right) \times C_m \tag{7}$$

2.4. Solution strategy

The Comsol Multiphysics 5.5 finite element software package is been utilized to solve the computational domain. A set of unstructured tetrahedral mesh is generated to discretize the domain. To minimize the uncertainty of simulations a grid independence test is carried out. The voltage and von Mises stress values for various tested total elements numbers are evaluated and tabulated in Table 3.

Table 3
Mesh independence test results for various element numbers.

Number of meshes	Voltage	Output Power	Maximum Von Mises stress
31485	0.05891900	0.01387741	68.95500000
65553.00	0.05891900	0.01387724	66.60500000
82061.00	0.05891900	0.01387724	101.43000000
105201.00	0.05891800	0.01387659	90.63500000
126892.00	0.05891700	0.01387620	91.79500000

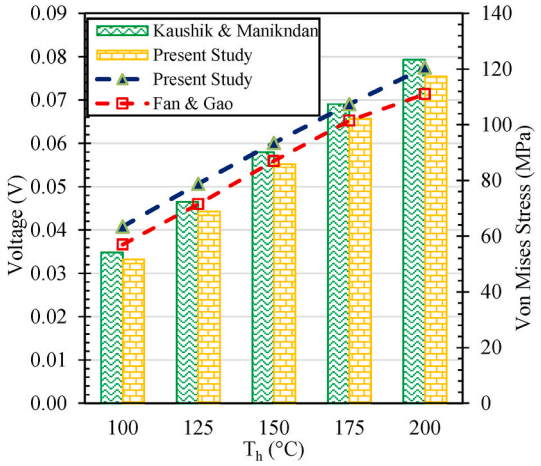

Fig. 2. Comparison of voltage and Von Mises stress between the presents study and literature.

As can be seen, the variation of energy analysis results with mesh numbers is minor while the mesh independence for mechanical study can be achieved for the number of elements around $1e^5$ and thus the simulations are carried out according to this mesh quality. The modelling and numerical methods are further verified by comparison of output voltage and von Mises stress with the results found in the literature. The numerical setting, parameters, material properties, and boundary conditions are set according to references i.e. constant temperature in both cold side and hot side while other boundaries are isolated. From mechanical viewpoint, the hot side is fixed and the cold side is free. As depicted in Fig. 2 the results of this study are in good agreement with those reported by Kausik and Manikandan [22] for voltage and Fan and Gao [18] for stress. A maximum difference of 4.91% and 10.74% can be reported for voltage and stress values between the results of the this paper and previous investigations.

3. Results and discussions

3.1. Energy results

The impact of leg cross section shape on power output and conversion efficiency under different heat fluxes is illustrated on Fig. 3 (the cold side temperature is fixed on 25°C). It can be seen that the triangular cross-section provides higher output power and conversion efficiency for all tested heal fluxes. It is remarkable that, the increment rate of output power (due to the increment of heat flux) in triangular cross-section is sharper compared the other cross-sections which shows the suitability of triangular shape for higher range

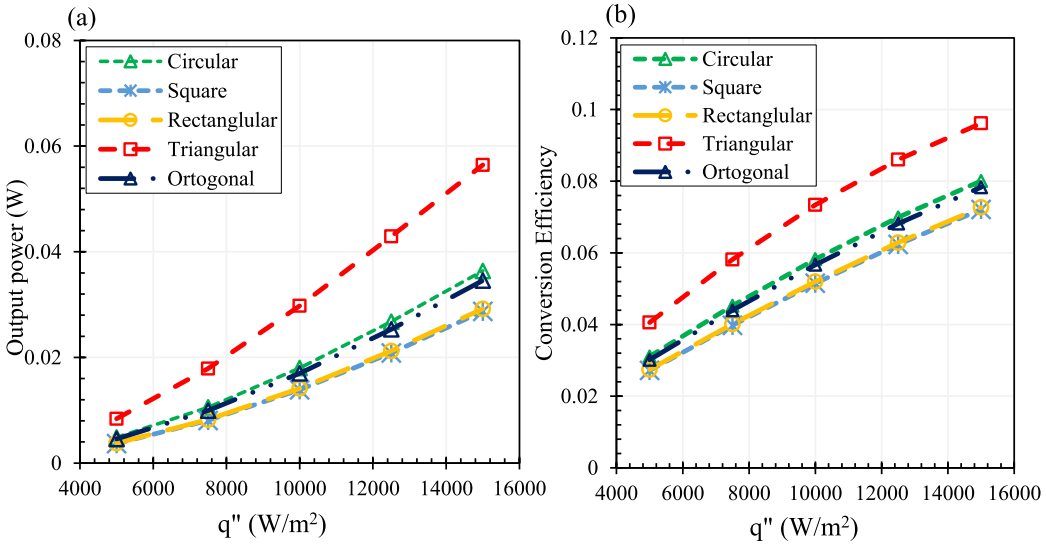

Fig. 3. a) Impact of leg cross section on output power at various heat fluxes and b) Impact of leg cross section on conversion efficiency at various heat fluxes.

heat fluxes. The generated power of triangular shape leg thermoelectric generators enhances by 655.5% with the increase of heat input flux from 5000 to 15000. The minimum output power belongs to rectangular and circular cross-sections. From generated power viewpoint, the best order of the cross-sections are triangular, circular, orthogonal, rectangular and square shape. At maximum input heat flux, the triangular cross-section is able to generate up to 100% higher output power compared to the square or rectangular cross-sections.

The order of conversion efficiency for all tested cross-sections is the same as output power i.e. the triangular cross section provides higher conversion efficiency. However, unlike the output power, the curves of convection efficiency is concave downward. It is also clear that, higher heat flux provides higher output power and conversion efficiency for all cross section shapes.

The impact of leg cross section on output power and conversion efficiency are also investigated under different cold side temperatures (heat flux is constant on 10000 W/m2) as illustrated in Fig. 4. Cold side temperature is varied between 25°C and 50°C. Increment of the cold side temperature of thermoelectric generator reduces the DC voltage and output power of the device because a smaller temperature gradient along the legs. Similar to Fig. 3, triangular cross section generates more power for all range of tested cold side temperatures.

25°C increase of temperature on the cold side of thermoelectric generator causes a 12.6% and 14.3% reduction in power generation of the system for circular and triangular shape leg thermoelectric, respectively. It can be seen in Fig. 4 (b) that the reduction of output power reflects on the conversion efficiency of the TEGs and lower efficiency values are obtained when cold side temperature increases. For the same 25°C amount of increment of cold side temperature, 10.1% and 21.4% reduction of conversion efficiency can be reported for circular and triangular shape leg thermoelectric, respectively.

For hollow leg structure the ratio of inner hollow area to total area is defined as $R_A = \frac{A_i}{A_0}$. Where A_0 is the base area of shapes in filled condition and A_i is the area of the inner hollow section. For instance the $R_A = 0.9$ corresponds to a study case in which 90% of leg volume is cut from inside. Fig. 5 depicts the effect of R_A on the maximum output power and conversion efficiency. As can be seen, with the increase of R_A the amount of power generation in the system increases. The higher values of R_A means thinner legs and the lesser volume of legs. With the increase of R_A, the internal resistance of the system decreases because the internal resistance of the thermoelectric devices has an inverse relation with the cross-sectional area of the legs and that is why with the increase of R_A higher electric current and output power are expected. Additionally, as results indicate, the TEG with the triangular shape legs produces more power and the least amount of power is generated with conventional square shape legs.

3.2. Exergy results

The exergy efficiency of a thermoelectric generator is a function of output power and has an inverse relation with input exergy which is applied to the device by heat [27–31]. The impact of leg cross-section shape on exergy efficiency under different heat fluxes and different cold side temperatures are presented in Fig. 6 (a) and Fig. 6 (b).

According to Fig. 6, triangular cross section provides higher exergy efficiency as well. However, when the cold side temperature is increases all cross sections (except square) give roughly the same amount of exergy efficiency (See Fig. 6 (b)). In other words, the significance of leg cross section shape is further highlighted when the cold side temperature is low. The results indicate that with the increase of cold side temperature the output power of TEGs decreases while the input exergy grows. It is expected that the combined effects caused by these two parameters lead to the reduction of exergy efficiency even by higher amounts compared to output power. Hence, a 25°C increase of temperature on the cold side reduces the exergy efficiency of circular and triangular shape leg TEGs by 26.7%

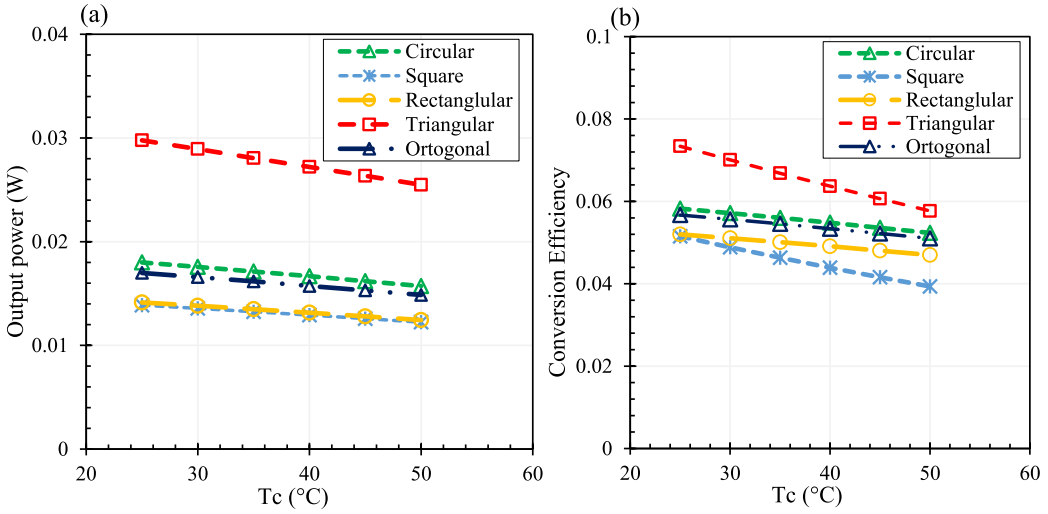

Fig. 4. Impact of leg cross section on a) output power at various cold side temperatures and b) on conversion efficiency at various cold side temperatures (heat flux = 10000 W/m^2).

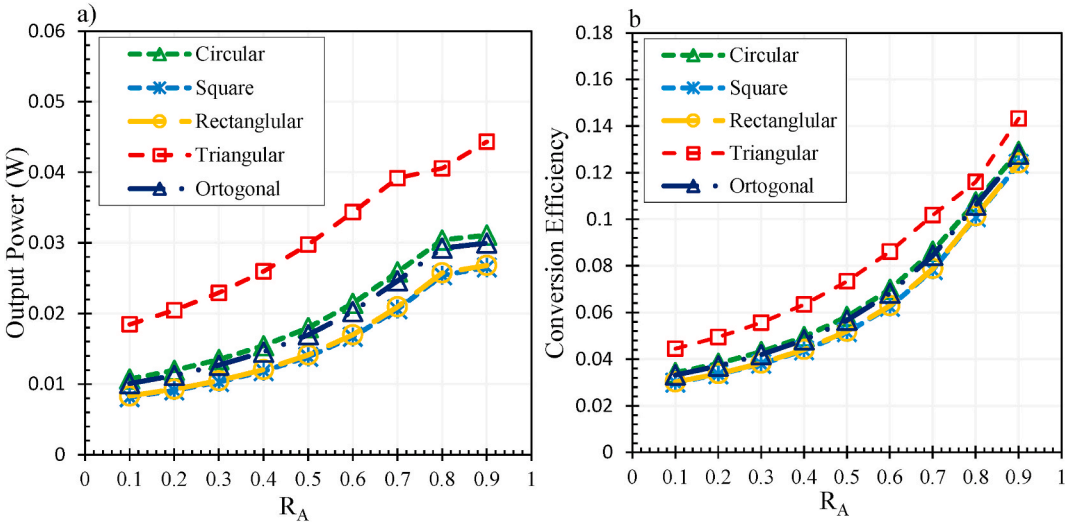

Fig. 5. The effect of ratio of inner hallow area to total area (R_A) on (a) power generation (b) conversion efficiency (heat flux = 10000 W/m^2).

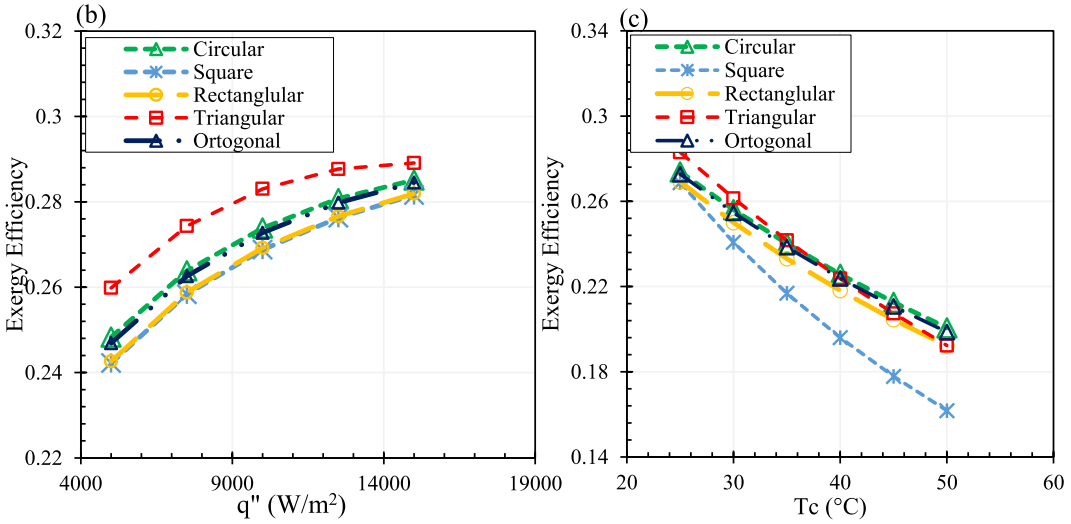

Fig. 6. a) Impact of leg cross section on exergy efficiency under different heat fluxes and b) Impact of leg cross section on exergy efficiency under different cold side temperatures (heat flux = 10000 W/m^2).

and 32% respectively.

3.3. Mechanical results

Being am appropriate cross-section from power output viewpoint, does not necessarily justifies its suitability from mechanical or economic point of views. Fig. 7 (a) and Fig. 7 (b) show the maximum Von-Misses stress under different heat fluxes (while cold side temperature is constant) and under different cold side temperature (while the heat flux is constant) respectively. According to Fig. 7, the created stress in triangular cross sections is higher than other cross sections for all ranges of heat fluxes and cold side temperatures. With increment of input heat flux, the intensity of the stress in triangular cross section is further enhanced. Circular cross section causes the smallest stress. At the minimum tested heat flux, the triangular shape causes 60% higher strass compared to the circular shape. However, the mentioned value is increased up to 100% when the input power is increased to its maximum value. The circular shape leg thermoelectric generator is the most mechanically reliable design.

Additionally, the von Mises stress test results depicted in Fig. 6(b) indicate that the increase of cold side temperature has a negative impact on the mechanical reliability of the system. For instance, 29.14% and 17.76% more stress is created in square shape and triangular shape legs by the increase of cold side temperature from 25°C to 50°C.

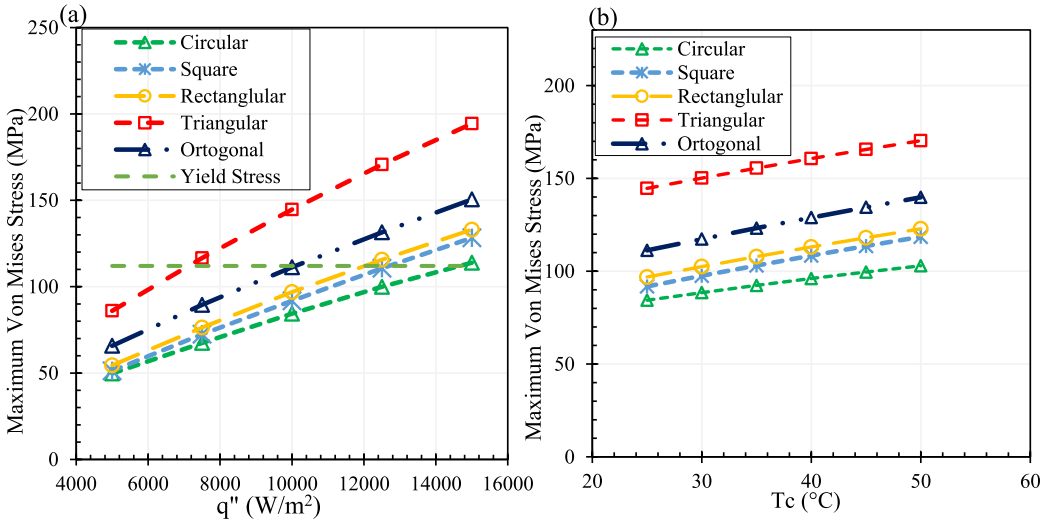

Fig. 7. a) Impact of leg cross section on Von Misses Stress under different heat fluxes and b) Impact of leg cross section on Von Misses Stress under different cold side temperatures.

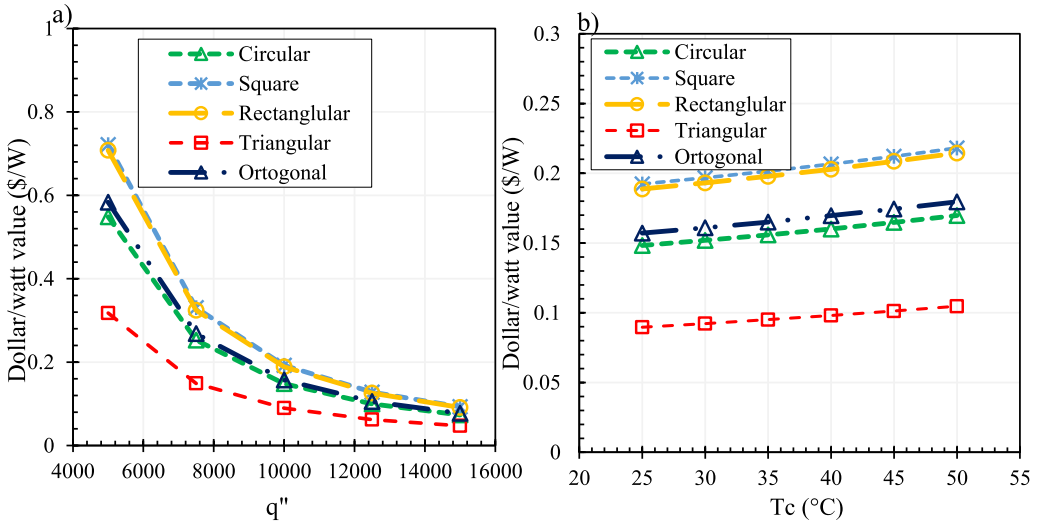

Fig. 8. a) Impact of leg cross section on Dollar/Watt value under different heat fluxes and b) Impact of leg cross section on Dollar/Watt value under different cold side temperatures.

3.4. Economic results

As thermoelectric generator is employed in solar systems and heat recovery process and son on [32–36], economic analysis would be a significant parameter. Fig. 8(a) depicts the changes in the dollar/watt value of the TEGs with input heat flux for all cross-section shapes. As discussed in the modelling section the dollar/watt value of any thermoelectric system is a function of output power and volumetric costs of materials. In this section, the volumetric costs of materials do not vary and thus it is expected that the dollar/watt value of the system decrease with the increase of input heat flux and output power. As shown the triangular shape leg thermoelectric generator produces more power per dollar of investment. An approximate 85% reduction in price per watt of output power can be reported when the input heat flux grows from 5000 to 15000. Fig. 8(b) depicts the changes in dollar/watt value of thermoelectric generators with various cross-sectional shapes versus the variation of cold side temperature. As can be seen, there is a 15% increase in costs per unit of output power for all of the geometries when temperature grows from 25°C to 50°C. As the volume of legs is constant the increase of dollar/watt values is due to the reduction of output power. The highest amount of increase of dollar watt value versus cold side temperature increment can be reported for triangular shape leg thermoelectric generator which is 16.8%.

4. Conclusion

In this paper, a three dimensional model of a thermoelectric generator with a hollow ring shape leg was proposed and the performance of various cross-sectional geometries including circular, square, rectangular, octagonal, and triangular on the power generation, energy/exergy efficiency, von Mises stress, and dollar/watt value of the device were investigated. The notable findings of the present study can be listed as follow:

- The triangular shape leg thermoelectric generator produces more power and has better conversion/exergy efficiency values while it causes the highest amount of von Mises stress, and thus it is a mechanically less reliable design. Also, results proved that the dollar/watt value of output power for triangular shape leg thermoelectric generator is less than other shapes.
- Applying more heat to TEGs can enhance the power generation, conversion/exergy efficiency, and reduces the cost of output power for all types of cross-sectional geometries but the mechanical limits caused by higher created thermal stresses in the leg should be carefully considered.
- The increase of cold side temperature has a negative impact on all of the tested performance criteria for all cross-sectional shapes.
- At the minimum tested heat flux, the triangular shape causes 60% higher strass compared to the circular shape. However, the mentioned value is increased up to 100% when the input power is increased to its maximum value.

CRediT authorship contribution statement

Min Li: Conceptualization, Resources, Formal analysis, Methodology. **Hamed Sadighi Dizaji:** Writing – original draft, Investigation. **Soheil Asaadi:** Software, Validation, Data curation. **Fahd Jarad:** Writing – review & editing, Resources. **Ali E. Anqi:** Writing – review & editing, Funding acquisition. **Makatar Wae-hayee:** Project administration.

Declaration of competing interest

The authors declare that they have no known competing financial interests or personal relationships that could have appeared to influence the work reported in this paper.

Acknowledgment

The authors extend their appreciation to the Deanship of Scientific Research at King Khalid University for the support they received through research groups program under grant number (R.G.P 2/138/42).

References

[1] S.M. Pourkiaei, M.H. Ahmadi, M. Sadeghzadeh, S. Moosavi, F. Pourfayaz, L. Chen, et al., Thermoelectric cooler and thermoelectric generator devices: a review of present and potential applications, modeling and materials, Energy 186 (2019) 115849, https://doi.org/10.1016/j.energy.2019.07.179.
[2] X.F. Zheng, C.X. Liu, Y.Y. Yan, Q. Wang, A review of thermoelectrics research – recent developments and potentials for sustainable and renewable energy applications, Renew. Sustain. Energy Rev. 32 (2014) 486–503, https://doi.org/10.1016/j.rser.2013.12.053.
[3] S. Shittu, G. Li, X. Zhao, X. Ma, Review of thermoelectric geometry and structure optimization for performance enhancement, Appl. Energy 268 (2020) 115075, https://doi.org/10.1016/j.apenergy.2020.115075.
[4] J. Dongxu, W. Zhongbao, J. Pou, S. Mazzoni, S. Rajoo, A. Romagnoli, Geometry optimization of thermoelectric modules: simulation and experimental study, Energy Convers. Manag. 195 (2019) 236–243, https://doi.org/10.1016/j.enconman.2019.05.003.
[5] A.Z. Sahin, B.S. Yilbas, The thermoelement as thermoelectric power generator: effect of leg geometry on the efficiency and power generation, Energy Convers. Manag. 65 (2013) 26–32, https://doi.org/10.1016/j.enconman.2012.07.020.
[6] A.S. Al-Merbati, B.S. Yilbas, A.Z. Sahin, Thermodynamics and thermal stress analysis of thermoelectric power generator: influence of pin geometry on device performance, Appl. Therm. Eng. 50 (2013) 683–692, https://doi.org/10.1016/j.applthermaleng.2012.07.021.
[7] R. Lamba, S.C. Kaushik, Thermodynamic analysis of thermoelectric generator including influence of Thomson effect and leg geometry configuration, Energy Convers. Manag. 144 (2017) 388–398, https://doi.org/10.1016/j.enconman.2017.04.069.
[8] B.S. Yilbas, S.S. Akhtar, A.Z. Sahin, Thermal and stress analyses in thermoelectric generator with tapered and rectangular pin configurations, Energy 114 (2016) 52–63, https://doi.org/10.1016/j.energy.2016.07.168.
[9] L. Zhu, H. Li, S. Chen, X. Tian, X. Kang, X. Jiang, S. Qiu, Optimization analysis of a segmented thermoelectric generator based on genetic algorithm, Renew. Energy 156 (2020) 710–718.
[10] S. Fan, Y. Gao, A. Rezania, Thermoelectric performance and stress analysis on wearable thermoelectric generator under bending load, Renew. Energy 173 (2021) 581–595.
[11] X. Su, L. Zhang, Z. Liu, Y. Luo, D. Chen, W. Li, Performance evaluation of a novel building envelope integrated with thermoelectric cooler and radiative sky cooler, Renew. Energy 171 (2021) 1061–1078.
[12] D. Luo, Y. Yan, R. Wang, W. Zhou, Numerical investigation on the dynamic response characteristics of a thermoelectric generator module under transient temperature excitations, Renew. Energy 170 (2021) 811–823.
[13] C.C. Maduabuchi, K.A. Ejenakevwe, C.A. Mgbemene, Performance optimization and thermodynamic analysis of irreversibility in a contemporary solar thermoelectric generator, Renew. Energy 168 (2021) 1189–1206.
[14] S.M. Borhani, M.J. Hosseini, R. Pakrouh, A.A. Ranjbar, A. Nourian, Performance enhancement of a thermoelectric harvester with a PCM/Metal foam composite, Renew. Energy 168 (2021) 1122–1140.
[15] Y. Thimont, S. LeBlanc, The impact of thermoelectric leg geometries on thermal resistance and power output, J. Appl. Phys. 126 (2019) 95101, https://doi.org/10.1063/1.5115044.
[16] U. Erturun, K. Mossi, Thermoelectric devices with rotated and coaxial leg configurations: numerical analysis of performance, Appl. Therm. Eng. 85 (2015) 304–312, https://doi.org/10.1016/j.applthermaleng.2015.04.010.
[17] S. Shittu, G. Li, X. Tang, X. Zhao, X. Ma, A. Badiei, Analysis of thermoelectric geometry in a concentrated photovoltaic-thermoelectric under varying weather conditions, Energy 202 (2020) 117742, https://doi.org/10.1016/j.energy.2020.117742.

[18] S. Fan, Y. Gao, Numerical simulation on thermoelectric and mechanical performance of annular thermoelectric generator, Energy 150 (2018) 38–48, https://doi.org/10.1016/j.energy.2018.02.124.
[19] T. Gong, Y. Wu, L. Gao, L. Zhang, J. Li, T. Ming, Thermo-mechanical analysis on a compact thermoelectric cooler, Energy 172 (2019) 1211–1224, https://doi.org/10.1016/j.energy.2019.02.014.
[20] S. Shittu, G. Li, Q. Xuan, X. Zhao, X. Ma, Y. Cui, Electrical and mechanical analysis of a segmented solar thermoelectric generator under non-uniform heat flux, Energy 199 (2020) 117433, https://doi.org/10.1016/j.energy.2020.117433.
[21] D.M. Rowe, Thermoelectrics Handbook: Macro to Nano, CRC Press, 2018.
[22] S.C. Kaushik, S. Manikandan, The influence of Thomson effect in the energy and exergy efficiency of an annular thermoelectric generator, Energy Convers. Manag. 103 (2015) 200–207.
[23] M.-W. Tian, L.W.W. Mihardjo, H. Moria, S. Asaadi, H. Sadighi Dizaji, S. Khalilarya, et al., A comprehensive energy efficiency study of segmented annular thermoelectric generator; thermal, exergetic and economic analysis, Appl. Therm. Eng. 181 (2020) 115996, https://doi.org/10.1016/j.applthermaleng.2020.115996.
[24] S.C. Kaushik, S. Manikandan, The influence of Thomson effect in the energy and exergy efficiency of an annular thermoelectric generator, Energy Convers. Manag. 103 (2015) 200–207, https://doi.org/10.1016/j.enconman.2015.06.037.
[25] S. Twaha, J. Zhu, Y. Yan, B. Li, A comprehensive review of thermoelectric technology: materials, applications, modelling and performance improvement, Renew. Sustain. Energy Rev. 65 (2016) 698–726, https://doi.org/10.1016/j.rser.2016.07.034.
[26] M.W. Tian, L.W. Mihardjo, H. Moria, S. Asaadi, S. Pourhedayat, H.S. Dizaji, M. Wae-hayee, Economy, energy, exergy and mechanical study of co-axial ring shape configuration of legs as a novel structure for cylindrical thermoelectric generator, Appl. Therm. Eng. 184 (2021) 116274.
[27] H.S. Dizaji, S. Jafarmadar, S. Khalilarya, S. Pourhedayat, A comprehensive exergy analysis of a prototype Peltier air-cooler; experimental investigation, Renew. Energy 131 (2019) 308–317.
[28] H. Moria, S. Pourhedayat, H.S. Dizaji, A.M. Abusorrah, N.H. Abu-Hamdeh, M. Wae-hayee, Exergoeconomic analysis of a Peltier effect air cooler using experimental data, Appl. Therm. Eng. 186 (2021) 116513.
[29] Y. Cao, N.H. Abu-Hamdeh, H. Moria, S. Asaadi, R. Alsulami, H.S. Dizaji, A novel proposed flexible thin-film solar annular thermoelectric generator, Appl. Therm. Eng. 183 (2021) 116245.
[30] M.W. Tian, H. Moria, L.W. Mihardjo, A. Kaood, H.S. Dizaji, K. Jermsittiparsert, Experimental thermal/economic/exergetic evaluation of hot/cold water production process by thermoelectricity, J. Clean. Prod. 271 (2020) 122923.
[31] S.R. Yan, H. Moria, S. Asaadi, H.S. Dizaji, S. Khalilarya, K. Jermsittiparsert, Performance and profit analysis of thermoelectric power generators mounted on channels with different cross-sectional shapes, Appl. Therm. Eng. 176 (2020) 115455.
[32] H.S. Dizaji, S. Jafarmadar, S. Khalilarya, Novel experiments on COP improvement of thermoelectric air coolers, Energy Convers. Manag. 187 (2019) 328–338.
[33] H.S. Dizaji, S. Jafarmadar, S. Khalilarya, A. Moosavi, An exhaustive experimental study of a novel air-water based thermoelectric cooling unit, Appl. Energy 181 (2016) 357–366.
[34] W. Li, M.C. Paul, J. Siviter, A. Montecucco, A.R. Knox, T. Sweet, G. Min, H. Baig, T.K. Mallick, G. Han, D.H. Gregory, Thermal performance of two heat exchangers for thermoelectric generators, Case studies in thermal engineering 8 (2016) 164–175.
[35] B.M. Fotso, R.C. Talawo, M.F. Nguefack, M. Fogue, Modeling and thermal analysis of a solar thermoelectric generator with vortex tube for hybrid vehicle, Case Studies in Thermal Engineering 15 (2019) 100515.
[36] Z.B. Tang, Y.D. Deng, C.Q. Su, W.W. Shuai, C.J. Xie, A research on thermoelectric generator's electrical performance under temperature mismatch conditions for automotive waste heat recovery system, Case Studies in Thermal Engineering 5 (2015) 143–150.